

Characterization of Ni₃Al Alloy Fabricated by Thermal Explosion/Hot Extrusion Technique

Liyuan SHENG^{1*}, Beining DU¹, Shaoping ZAN², Junke JIAO²

¹ Shenzhen Institute, Peking University, Shenzhen 518057, China

² Ningbo Institute of Materials Technology and Engineering, Chinese Academy of Sciences Ningbo, 315201, China

crossref <http://dx.doi.org/10.5755/j01.ms.24.4.19460>

Received 10 November 2017; accepted 13 January 2018

In the present paper, the trace B doped Ni₃Al alloy was prepared by the thermal explosion and hot extrusion (TH/HE) technique. Its microstructure characterization and mechanical properties were carried out by OM, XRD, TEM, compression and microhardness tests. Microstructure examinations exhibit that the TH/HE technology has transformed the powders into Ni₃Al alloy with less porosity. In the synthesized part, coarse and ultrafine Ni₃Al grains constitute the dual-scale grain structure with segregated Al₂O₃ particles along grain boundary. TEM observations reveal that γ -Ni, Al₂O₃ and Ni₃Al phases coexist in the synthesized part. Moreover, the Al₂O₃ particles in the synthesized part have α -Al₂O₃ and γ -Al₂O₃ two crystal structures. In addition, there is a transition region along the interface of Al₂O₃ and Ni₃Al grain. The subsequent hot extrusion optimizes the microstructure of the extruded part by homogenizing the Ni₃Al grain, uniformly distributing Al₂O₃ and generating massive substructures. The great deformation results in the pile-up of dislocations, intersected dislocations and substructures. Moreover, the movement of dislocation promotes the formation of micro-twinning in the Ni₃Al grain, which is accompanied with the stacking faults and nano-structure. The mechanical properties exhibit that the microstructure optimization caused by the TE/HE technique improves the compressive ductility and strength of the Ni₃Al alloy obviously.

Keywords: Ni₃Al, thermal explosion, hot extrusion, microstructure, mechanical properties.

1. INTRODUCTION*

Intermetallic compounds are the kind of materials which possess the special properties in some aspects, so they have been paid much attention and many researches have been carried out [1–4]. As a kind of intermetallic compound, Ni₃Al attracted so much attention due to its excellent properties at high temperature, such as high melting point, good creep resistance, excellent corrosion and oxidation resistance [5–7]. Therefore, it has been considered as a promising structure material to use in aircraft engine [8]. Despite of these attractive advantages, the brittle fracture, processing problem and low ductility of the Ni₃Al are the major difficulties that handicap its wide application [9, 10]. In order to solve these key problems, many methods have been applied and many kinds of Ni₃Al based alloys [11–13].

The previous research of Liu exhibited that the trace addition of B could improve the ductility of the Ni₃Al greatly with 24 % (at.%) Al [14]. While the research on the Ni₃Al revealed that the moisture environment resulted the embrittlement of the Ni₃Al [15]. Therefore, the addition of B would resist the influence of moisture on the grain boundary of Ni₃Al and improve its ductility. Though the B addition in Ni₃Al could increase its ductility, however its yield strength still not high enough. According to the recent investigations [16–18], the microstructure refinement was a convenient way to increase the strength without detrimental to the ductility. Previously, the study on the Ni₃Al alloy exhibited its mechanical properties

could be improved further by the grain refinement and dispersoid particles [7, 19]. Among the material processing technologies, the powder metallurgy is recognized as an attractive method to fabricate the Ni₃Al alloy with strengthening particles, because of its advantages of microstructure refinement and near-net forming [20, 21]. The research of Yeh exhibited that the Ni₃Al alloy could be fabricated by self-propagating synthesis [22]. While the A. Antolak-Dudka et al. [23] fabricated the bulk nanocrystalline Ni₃Al alloys by hot-pressing consolidation of mechanically alloyed powders. However, the researches of Sheng [12, 18, 24] revealed that there was porosity in the Ni₃Al or NiAl based alloy prepared by powder metallurgy. In general, the fabricated specimen by powder metallurgy would be treated with hot isostatic pressing (HIP), but it would result in the coarsening of microstructure. The recent studies [12, 20] demonstrated that the hot extrusion following the synthesis could densify the specimen and decrease the porosity obviously. In addition, based on the former research [14], the addition of 0.2–1 % (at.%) boron should be appropriate selection, which had the optimal improvement on the ductility. Therefore, in the present research, the thermal explosion and hot extrusion (TE/HE) is employed to fabricate the Ni₃Al alloy with 0.3 % (at.%) boron addition. Its microstructure is characterized by the transmission electron microscopy and its mechanical properties are analyzed as well.

2. EXPERIMENTAL DETAILS

The elemental nickel powder (with an average size of 0.9 μ m), aluminum powder (1.5 μ m) and boron powder

* Corresponding author. Tel.: +86-755-26984814; fax: +86-755-26737080. E-mail address: lysheng@yeah.net (L.Y. Sheng)

(3 μm) were used as the initial materials. These powders (Ni:Al:B = 74.7:25:0.3, atomic ratio) were dry mixed by the ball milling for three hours. The mixed powders were put into the TE/HE synthesis system, as shown in Fig. 1 a. The powders were compacted by the puncheon to get a relative densified sample. Then the densified sample was heated by induction coil rapidly to 760 K to ignite the reaction synthesis. During the heating and synthesis, the thermocouple in the TE/HE synthesis system was used to detect the temperature of the compacted powders. When the detected temperature was higher than 2000 K, it indicated the reaction synthesis had begun. Then, a force of 400 MPa would be exerted on the reaction puncheon to extrude the synthesized Ni_3Al out of the reaction floor through a hole with the diameter of 6 mm. During the extrusion, a back force was exerted on the extruded part to ensure its compactness. The as fabricated sample is shown in Fig. 1 b.

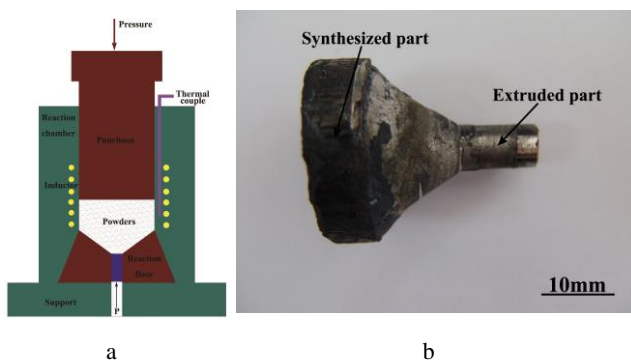


Fig. 1. a–schematic diagram of the thermal explosion and hot extrusion synthesis system; b–appearance of the synthesized sample

Specimens for microstructure characterization and mechanical properties tests were cut from the synthesized part and extruded part. The OLYMPUS GX41 optical microscope (OM) was used to perform microstructure characterization. The specimen for OM observation was prepared by mechanical polishing and chemical etching with the acidic mixture ($\text{CH}_3\text{COOH}/\text{HNO}_3/\text{HCl}=8:4:1$). The resultant phases in the Ni_3Al alloy were analyzed by X-ray diffraction (XRD) with a Cu radiation at 40 kV and 40 mA. JEOL-2100 high-resolution transmission electron microscope (TEM) was employed to carry out the TEM characterization and the specimen was cut from alloy with the thickness of 0.4 mm. Then the specimen was polished to 30 μm and shaped into $\phi 3$ mm in size followed by twin-jet electropolishing. Due to the small size of the synthesized sample, compression test and microhardness were adopted to evaluate its mechanical properties. Compression sample (4 mm \times 4 mm \times 6 mm) was cut from the synthesized sample and mechanically grounded by 800-grit SiC abrasive. Gleeble 1500 was employed to carry out the compression test at the strain rate of $1 \times 10^{-3}/\text{s}$. Hardness evaluation was performed on the HV-1000 Vicker microhardness tester with dwell time of 20 s and load of 150 g.

3. RESULTS AND DISCUSSION

3.1. Microstructure characteristics

The Ni_3Al alloy with trace B addition was successfully fabricated by TE/HE technique. The X-ray diffraction pattern of the Ni_3Al alloy is analyzed based on the powder diffraction data of Ni_3Al structure (JCPDS 65-0144) [25], as shown in Fig. 2 a. Clearly, the elemental powders have fully reacted and been transformed into Ni_3Al phase by the TE/HE process. Moreover, it can find that the Ni_3Al prefers to grow along the (111) crystal plane. Except the Ni_3Al phase, just a little peak of Al_2O_3 phase can be found in the X-ray diffraction pattern. OM image of the synthesized part and the extruded part of the TE/HE synthesized Ni_3Al alloy are shown in Fig. 2 b and c, respectively.

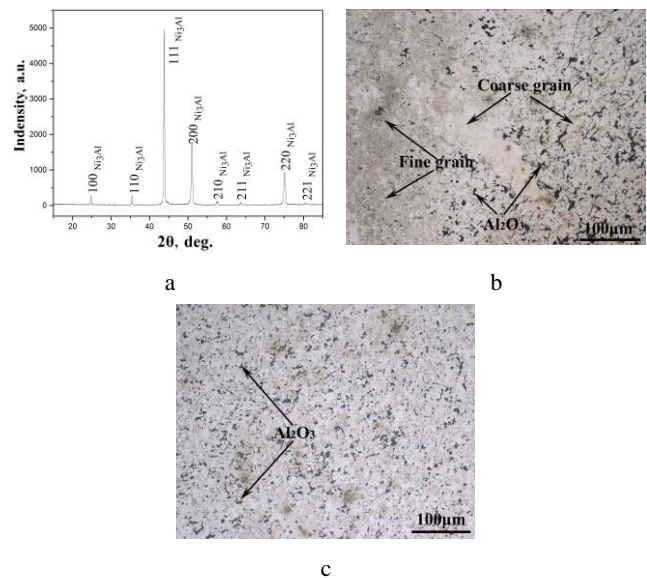


Fig. 2. a–X-ray diffraction patterns of Ni_3Al alloy prepared by TE/HE; b–OM image of the synthesized part; c–OM image of the extruded part

Both parts of the synthesized alloy are well compacted with low porosity, but the extruded part has more homogeneous microstructure than the synthesized part. In the synthesized part, there are multiscale grains with grain size from 10 μm to 100 μm . In the marginal region of the synthesized part, the ultrafine grain less than 5 μm is the main feature, which may be ascribed to the high cooling rate resulted by the mould of TE/HE synthesis system. With the region approaching to the centre of synthesized part, the microstructure becomes coarse and dual-scale grains appear. The coexistence of coarse and fine grains should be attributed to the high reaction temperature and low heat transfer rate, because the marginal region restrains the heat transfers rapidly. The residual heat promotes the growth of the Ni_3Al grain. Due to the competition of grain growth, some ones grow rapidly and become the coarse grain. In the region far from the margin, the microstructure is mainly composed of dual-scale grain and Al_2O_3 particles. Moreover, it can be found that the Al_2O_3 particles mainly distribute on the grain boundaries, but some agglomerate obviously. In the extruded part, the grain is homogeneous with the average size of 10 μm . The

Al_2O_3 particle in the extruded part is fine and distributes uniformly. The gross statistics on the Al_2O_3 particles in the synthesized Ni_3Al alloy indicates its volume percent is about 4%. The formation of Al_2O_3 particles should be ascribed to oxidation during the powders milling and thermal explosion process, because the TE/HE system have no protective atmosphere. The oxygen could infiltrate into the green compact during the initial compacting. Then the Al_2O_3 dispersoids would be generated due to its priority [26]. The presence of Al_2O_3 dispersoids is beneficial to the microstructure refinement by forming necklace like precipitates along grain or phase boundary [27, 28].

The results of TEM observations on the synthesized part of the Ni_3Al alloys are presented in Fig. 3. Different from the OM observation, TEM analysis exhibits that the matrix contains nanostructure, as shown in Fig. 3 a. The ultrafine Ni_3Al grain has the size of hundreds of nanometers. Such refined microstructure may be partly attributed to the deformation induced by the following hot extrusion that forces the synthesized part to deform and promotes the subgrains. The selected area diffraction pattern (SADP) confirms the formation of the Al_2O_3 dispersoids, as shown in Fig. 3 b. The Al_2O_3 dispersoids prefer to distribute along the grain boundary, which could contribute to the grain refinement. The aggregated Al_2O_3 dispersoids in the matrix can generate the barrier effect, which prevents the growth of Ni_3Al grain at high temperature. Moreover, they are also helpful to the fragmentation of Ni_3Al phase, due to its high strength at high temperature. They would result in the pinning effect and separate the bulk Ni_3Al phase during the hot extrusion. The observations on the Al_2O_3 dispersoids aggregated region reveals the formation of γ -Ni phase, as shown in Fig. 3 c. Except the segregation of Ni powders, such a phenomenon should be ascribed to the reaction of oxygen with aluminum during the synthesis process, which causes the deficient of Al.

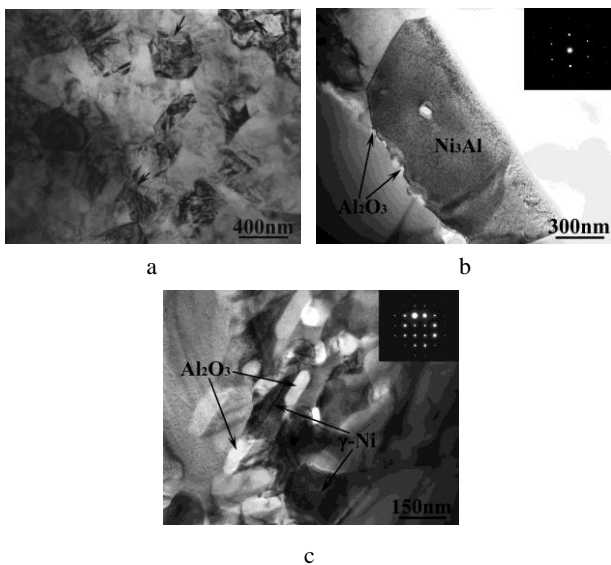


Fig. 3. a – TEM image of ultrafine Ni_3Al grains in the synthesized part; b – morphology of Al_2O_3 particles along grain boundary (Inset pictures show the SADP of Al_2O_3); c – formation of γ -Ni phase around Al_2O_3 particles (Inset pictures show the SADP γ -Ni)

TEM observations on the Al_2O_3 particles exhibit they contain two kinds of crystal structure, as shown in Fig. 4. The SADP has confirmed that one is α - Al_2O_3 with the hexagonal crystal structure ($a = b = 0.4758 \text{ nm}$, $c = 1.299 \text{ nm}$) and R3c space group, as shown in Fig. 4 a. Based on the recent research [29], the α - Al_2O_3 is the most stable phase in all Al_2O_3 crystals. The high-resolution TEM (HRTEM) observation on the interface of α - Al_2O_3 and Ni_3Al reveals that there is a transition area about several nanometers, as shown in Fig. 4 b. In the transition area, the atoms array changes a little compared with that in the center of α - Al_2O_3 . Combining SADP and TEM observations, the other Al_2O_3 is determined as the γ - Al_2O_3 with the face-centered crystal structure ($a = b = c = 0.7948 \text{ nm}$) and Fd3m space group, as shown in Fig. 4 c. The γ - Al_2O_3 is a metastable phase that would transform into α - Al_2O_3 during heat treatment. HRTEM observation on the interface of γ - Al_2O_3 exhibits that it has a zigzag pattern and contains interface dislocations, as shown in Fig. 4 d. Additionally, along the interface some subgrains start to form. The changes of the interface of Al_2O_3 should be ascribed to the great lattice difference. It is the rapid synthesis process that results in the presence of the two kinds of Al_2O_3 . During the synthesis, the high temperature and high pressure in the short time promote the formation of Al_2O_3 particles with the different structure, but the high cooling rate handicaps the phase transformation and reserve these Al_2O_3 crystals.

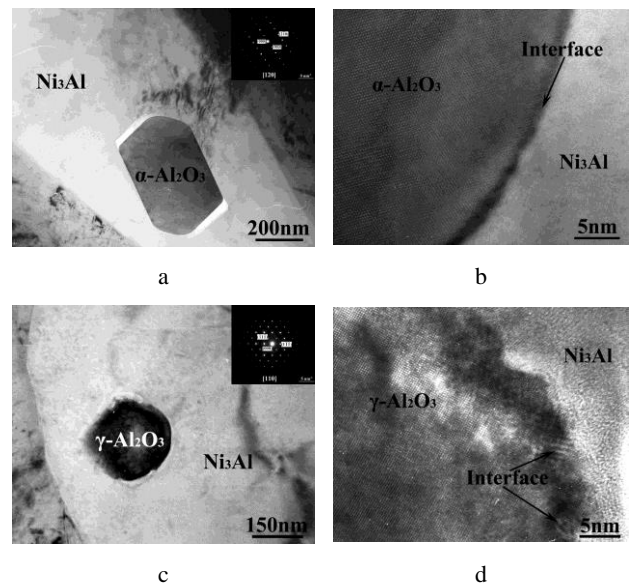


Fig. 4. a – bright-field TEM micrographs of the α - Al_2O_3 particle (Inset image showing the SADP of α - Al_2O_3 precipitate); b – HRTEM image of α - Al_2O_3 / Ni_3Al interface; c – bright-field TEM micrographs of the γ - Al_2O_3 particle (Inset image showing the SADP of γ - Al_2O_3 precipitate); d – HRTEM image of γ - Al_2O_3 / Ni_3Al interface

TEM observations on the extruded part of the TE/HE synthesized Ni_3Al alloy reveal that the Ni_3Al has experienced great deformation, as shown in Fig. 5 a. The hot extrusion process forces the Ni_3Al grain to extend along the extrusion direction, so some Ni_3Al phase exhibits long strip shape. Compared with the synthesized part, the grain size of the extruded part becomes finer, and the distribution of Al_2O_3 dispersoids becomes more

homogeneous. Then it can be deduced that the extrusion deformation and Al_2O_3 dispersoids work together results in the microstructure refinement. Due to the short time of TH/HE and great deformation, it is impossible for the alloy to have a recrystallization. Therefore, massive dislocations can be observed in the extruded part, as shown in Fig. 5 b. The dislocations intersect with each other along the grain boundary, which promotes the formation of the substructure. Obviously, the original grain boundary could effect as the barrier of the dislocations. It is difficult for the dislocations to traverse the grain boundary. In the bulk Ni_3Al grain, it still can find the dislocation arrays and their intersection, as shown in Fig. 5 c.

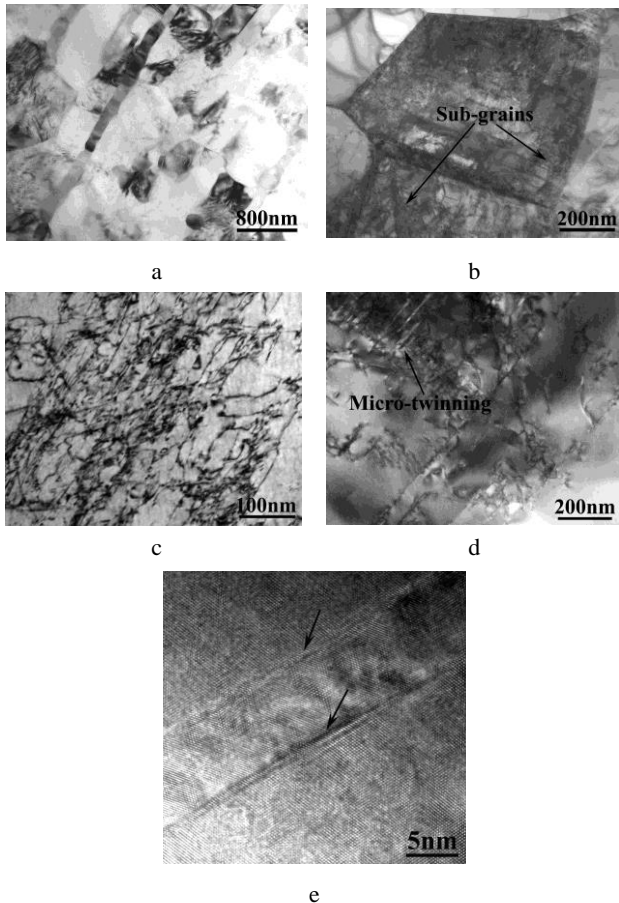


Fig. 5. a–TEM images of the extruded part showing the deformation of the Ni_3Al phase; b–irregular dislocations and subgrains along grain boundary; c–intersected dislocation arrays inside Ni_3Al grain; d–formation of microtwinning in Ni_3Al crystal promoted by dislocation; e–HRTEM of microtwinning boundary

Such intersected and tangled dislocations in the Ni_3Al grain should be attributed the great deformation during the extrusion process. Moreover, these dislocations are also beneficial to the strength and promote the crystal defects. As shown in Fig. 5 d, the micro-twinning is generating in the region with great pile-up dislocations and tangled dislocations. It is interesting that the twinning begins accompanied with the dislocations movement. HRTEM observation on the micro-twinning finds that stacking faults seems to form along the twinning boundary, as shown in Fig. 5 e. Near the micro-twinning region, it also can find that there are some substructures with several

nanometers. It indicates that the great deformation promotes micro-twinning and substructure as well. In general, the microstructure evolution of Ni_3Al alloy during TE/HE should be ascribed to the great deformation, short synthesis time and high cooling rate. The short synthesis time and high cooling rate result in the diversified structure and phase. So many kinds of phases reverse in the synthesized part. The great deformation during hot extrusion compels the alloy deforms along the extrusion direction, which would promote the anisotropic characteristic. Then many crystal defects generate in the alloy.

3.2. Mechanical properties

The room-temperature mechanical properties and microhardness of the TE/HE synthesized Ni_3Al alloy are shown in Table 1. Moreover, the mechanical properties of Ni_3Al alloy fabricated by combustion synthesis in former research [30] are also listed in the Table 1. From the data, one can find that the TE/HE process improves the mechanical properties of the Ni_3Al alloy obviously, especially the strength. The improvement should be ascribed to the microstructures optimization by the TE/HE process. The fine Ni_3Al grain, trace B addition, Al_2O_3 dispersoids and massive crystal defects all contribute to the mechanical properties. According the previous researches [8, 14, 31, 32], the trace B addition in the Ni_3Al alloy with 24 % (at.%) Al increased the ductility obviously by improving the cohesion of grain boundary. In the present research, though trace B is added in the Ni_3Al alloy, however the milling and thermal explosion would preserve the B in the grain [12, 33, 34]. Therefore, the grain boundary strengthening by the B is restrained. Moreover, the Al content of present research is 25 % (at.%), which influences the ductility improvement further. Additionally, the presence of Al_2O_3 dispersoids also exerts negative influence on the compressive ductility. The widely distributed Al_2O_3 particle in the TE/HE synthesized Ni_3Al alloy contributes to the strength, but its non-uniform distribution, especially the segregated Al_2O_3 dispersoids, would lead to great stress concentration and decrease its compressive ductility. Then it can be understood that the compressive ductility of TE/HE Ni_3Al alloy is not improved significantly, compared with the Ni_3Al alloy without B addition. However, the comparison of the synthesized part and extruded part of the TE/HE prepared Ni_3Al alloy exhibits that the subsequent hot extrusion increases the yield strength a little but enhances the compressive strain obviously. Based on the microstructure observation above, it can be find that the hot extrusion eliminates the dual-scale grain and homogenize the grain size. According to the former investigation [35–37], the dual-scale grains decrease the synchronization between grains during deformation, which may result in great dislocation accumulated in the coarse grain boundary and the crack initiation. The homogeneous grain in the part would be beneficial to the plastic deformation. In fact, the grain homogenization could be attributed to the presence of Al_2O_3 dispersoids partly. During the hot extrusion, the rheological behavior of Ni_3Al alloy compels the Ni_3Al grain to deform along the extrusion direction.

Table 1. Room-temperature mechanical properties and microhardness of the TE/HE synthesized Ni₃Al alloy and the combustion synthesized Ni₃Al alloys

Alloy	Yield strength, MPa	Compressive strength, MPa	Compressive strain, %	Microhardness, HV
Synthesized part	405	1350	23	280
Extruded part	450	1430	35	300
Ni ₃ Al [17]	230	680	15	220

The combination of grain torsion and pinning effect of Al₂O₃ dispersoids promote the fragmentation of bulk Ni₃Al grain in the neck of the mould. Moreover, the necklace distribution of Al₂O₃ dispersoids along grain boundary restrain the overgrowth of grain. In addition, the great amounts of dislocations and subgrains generated in the extruded part contribute much to the strength.

4. CONCLUSIONS

1. The trace B doped Ni₃Al alloy is prepared by the thermal explosion and hot extrusion synthesis technique. In the synthesized part, coarse and ultrafine Ni₃Al grains comprise the dual-scale grain structure with segregated Al₂O₃ particles along grain boundary. Moreover, the Al₂O₃ formed in the synthesized part contains α -Al₂O₃ and γ -Al₂O₃ two crystal structure, possessing a transition region along the interface.
2. The subsequent hot extrusion optimizes the microstructure of the extruded part by homogenizing the Ni₃Al grain, uniformly distributing Al₂O₃ and generating massive substructures. Moreover, the great deformation promotes dislocations movement and results in the formation of micro-twinning.
3. Compared with the combustion synthesized Ni₃Al alloy, the thermal explosion and hot extrusion synthesized Ni₃Al alloy owns better mechanical properties. Moreover, the extruded part possesses the highest compressive properties

Acknowledgments

The authors are grateful to the Shenzhen Technology Research Program (JSGG20170412145203293) and Shenzhen Basic Research Project (JCYJ20150529162228734, JCYJ 20160427170611414, JCYJ20160427100211076).

REFERENCES

1. **PoPe, D.P., Ezz, S.S.** Mechanical Properties of Ni₃Al and Nickel-base Alloys with High Volume Fraction of Gamma *International Metal Review* 29 (3) 1984: pp. 136–167. <https://doi.org/10.1179/imtr.1984.29.1.136>
2. **Sheng, L.Y., Yang, F., Xi, T.F., Zheng, Y.F., Guo, J.T.** Microstructure and Room Temperature Mechanical Properties of NiAl-Cr(Mo)-(Hf,Dy) Hypoeutectic Alloy Prepared by Injection Casting *Transaction Nonferrous Metal Society of China* 23 2013: pp. 983–990. [https://doi.org/10.1016/S1003-6326\(13\)62556-X](https://doi.org/10.1016/S1003-6326(13)62556-X)
3. **Ye, H.Q.** Recent Developments in High Temperature Intermetallics Research in China *Intermetallics* 8 2000: pp. 503–509. [https://doi.org/10.1016/S0966-9795\(99\)00132-6](https://doi.org/10.1016/S0966-9795(99)00132-6)

4. **Sheng, L.Y., Du, B.N., Lai, C., Guo, J.T., Xi, T.F.** Influence of Tantalum Addition on Microstructure and Mechanical Properties of the NiAl-Based Eutectic Alloy *Strength of Materials* 49 (1) 2017: pp. 109–117. <https://doi.org/10.1007/s11223-017-9848-6>
5. **Stoloff, N.S., Liu, C.T., Deevi, S.C.** Emerging Applications of Intermetallics *Intermetallics* 8 2000: pp. 1313–1320. [https://doi.org/10.1016/S0966-9795\(00\)00077-7](https://doi.org/10.1016/S0966-9795(00)00077-7)
6. **Sheng, L.Y., Xi, T.F., Lai, C., Guo, J.T., Zheng, Y.F.** Effect of Extrusion Process on Microstructure and Mechanical Properties of Ni₃Al-B-Cr Alloy during Self-propagation High-temperature Synthesis *Transaction Nonferrous Metal Society of China* 22 2012: pp. 489–495. [https://doi.org/10.1016/S1003-6326\(11\)61203-X](https://doi.org/10.1016/S1003-6326(11)61203-X)
7. **Sheng, L.Y., Yang, F., Xi, T.F., Guo, J.T., Ye, H.Q.** Microstructure Evolution and Mechanical Properties of Ni₃Al/Al₂O₃ Composite during Self-propagation High-Temperature Synthesis and Hot Extrusion *Materials Science Engineering A* 555 2012: pp. 131–138. <https://doi.org/10.1016/j.msea.2012.06.042>
8. **Stoloff, N.S.** Physical and Mechanical Metallurgy of Ni₃Al and Its Alloys *International Materials Reviews* 34 (1) 1989: pp. 153–184. <https://doi.org/10.1179/imr.1989.34.1.153>
9. **Liu, C.T.** Environmental Embrittlement and Grain-boundary Fracture in Ni₃Al *Scripta Metallurgica et Materialia* 27 (1) 1992: pp. 25–28. [https://doi.org/10.1016/0956-716X\(92\)90313-4](https://doi.org/10.1016/0956-716X(92)90313-4)
10. **Sheng, L.Y., Xie, Y., Xi, T.F., Guo, J.T., Zheng, Y.F., Ye, H.Q.** Microstructure Characteristics and Compressive Properties of NiAl-based Multiphase Alloy during Heat Treatments *Materials Science Engineering A* 528 (29–30) 2011: pp. 8324–8331. <https://doi.org/10.1016/j.msea.2011.07.072>
11. **Yeh, C.L., Sung, W.Y.** Combustion Synthesis of Ni₃Al by SHS with Boron Additions *Journal of Alloys and Compound* 390 2005: pp. 74–81. <https://doi.org/10.1016/j.jallcom.2004.08.025>
12. **Sheng, L.Y., Zhang, W., Guo, J.T., Wang, Z.S., Ovcharenko, V.E., Zhou, L.Z., Ye, H.Q.** Microstructure and Mechanical Properties of Ni₃Al Fabricated by Thermal Explosion and Hot Extrusion *Intermetallics* 17 2009: pp. 572–577. <https://doi.org/10.1016/j.intermet.2009.01.004>
13. **Wu, X.X., Wang, C.Y.** Effect of the Alloying Element on the Temperature-dependent Ideal Shear Strength of Gamma'-Ni₃Al *RSC Advances* 6 (25) 2016: pp. 20551–20558. <https://doi.org/10.1039/c5ra24108a>
14. **Liu, C.T., White, C.L., Horton, J.A.** Effect of Boron on Grain-boundaries in Ni₃Al *Acta Metallurgica* 33 1985: pp. 213–229. [https://doi.org/10.1016/0001-6160\(85\)90139-7](https://doi.org/10.1016/0001-6160(85)90139-7)
15. **George, E.P., Liu, C.T., Pope, D.P.** Intrinsic Ductility and Environmental Embrittlement of Binary Ni₃Al *Scripta Metallurgica et Materialia* 28 1993: pp. 857–862.

- [https://doi.org/10.1016/0956-716X\(93\)90366-Z](https://doi.org/10.1016/0956-716X(93)90366-Z)
16. **Sheng, L.Y., Lai, C., Yang, F., Wang, Q.L., Xi, T.F.** Microstructure and Wear Behaviour of Ceramic Particles Strengthening NiAl Based Composite *Materials Research Innovation* 18 (S4) 2014: pp. 544–549.
<https://doi.org/10.1179/1432891714Z.000000000738>
 17. **Demura, M., Suga, Y., Umezawa, O., Kishida, K., George, E.P., Hirano, T.** Fabrication of Ni₃Al Thin Foil by Cold-Rolling *Intermetallics* 9 2001: pp. 157–167.
[https://doi.org/10.1016/S0966-9795\(00\)00121-7](https://doi.org/10.1016/S0966-9795(00)00121-7)
 18. **Sheng, L.Y., Guo, J.T., Xi, T.F., Zhang, B.C., Ye, H.Q.** ZrO₂ Strengthened NiAl/Cr (Mo, Hf) Composite Fabricated by Powder Metallurgy *Progress in Natural Science: Materials International* 22 (3) 2012: pp. 231–236.
<https://doi.org/10.1016/j.pnsc.2012.04.003>
 19. **Schulson, E.M., Weihs, T.P., Viens, D.V., Baker, I.** The Effect of Grain Size on the Yield Strength of Ni₃Al *Acta Metallurgica* 33 1985: pp. 1587–1591.
[https://doi.org/10.1016/0001-6160\(85\)90152-X](https://doi.org/10.1016/0001-6160(85)90152-X)
 20. **Guo, J.T., Sheng, L.Y., Xie, Y., Zhang, Z.X., Ovcharenko, V.E., Ye, H.Q.** Microstructure and mechanical properties of Ni₃Al and Ni₃Al–1B alloys fabricated by SHS/HE *Intermetallics* 19 2011: pp. 137–142.
<https://doi.org/10.1016/j.intermet.2010.08.027>
 21. **Sheng, L.Y., Guo, J.T., Yuan, C., Yang, F., Li, G.S., Xi, T.F.** Investigation on B, Cr Doped Ni₃Al Alloy Prepared by Self-propagation High-temperature Synthesis and Hot Extrusion *Materials Science Forum* 747 2013: pp. 124–131.
<https://doi.org/10.4028/www.scientific.net/MSF.747-748.124>
 22. **Yeh, C.L., Sung, W.Y.** Combustion Synthesis of Ni₃Al Intermetallic Compound in Self-propagating Mode *Journal of Alloys and Compound* 384 (1–2) 2004: pp. 181–191.
<https://doi.org/10.1016/j.jallcom.2004.04.116>
 23. **Antolak-Dudka, A., Krasnowski, M., Kulik, T.** Nanocrystalline Ni₃Al Intermetallic Produced by Hot-Pressing Consolidation of Mechanically Alloyed Powders *Intermetallics* 42 2013: pp. 41–44.
<https://doi.org/10.1016/j.intermet.2013.05.014>
 24. **Sheng, L.Y., Yang, F., Guo, J.T., Xi, T.F., Ye, H.Q.** Investigation on NiAl-TiC-Al₂O₃ Composite Prepared by Self-propagation High Temperature Synthesis with Hot Extrusion *Composite Part B- Engineering* 45 2013: pp. 785–791.
<https://doi.org/10.1016/j.compositesb.2012.05.038>
 25. **Polkowski, W., Jozwik, P., Bojar, Z.** EBSD and X-ray Diffraction Study on the Recrystallization of Cold Rolled Ni₃Al Based Intermetallic Alloy *Journal of Alloys and Compounds* 614 2014: pp. 226–233.
<https://doi.org/10.1016/j.jallcom.2014.06.106>
 26. **Zhu, X., Zhang, T., Morris, V., Marchant, D.** Combustion Synthesis of NiAl/Al₂O₃ Composites by Induction Heating *Intermetallics* 18 (6) 2010: pp. 1197–1204.
<https://doi.org/10.1016/j.intermet.2010.03.009>
 27. **Sheng, L.Y., Yang, F., Xi, T.F., Zheng, Y.F., Guo, J.T.** Improvement of Compressive Strength and Ductility in NiAl-Cr(Nb)/Dy Alloy by Rapid Solidification and HIP Treatment *Intermetallics* 27 2012: pp. 14–20.
<https://doi.org/10.1016/j.intermet.2012.01.014>
 28. **Sheng, L.Y., Guo, J.T., Ren, W.L., Zhang, Z.X., Ren, Z.M., Ye, H.Q.** Preliminary Investigation on Strong Magnetic Field Treated NiAl-Cr(Mo)-Hf Near Eutectic Alloy *Intermetallics* 19 (2) 2011: pp. 143–148.
<https://doi.org/10.1016/j.intermet.2010.08.026>
 29. **Sheng, L.Y., Yang, F., Xi, T.F., Lai, C., Ye, H.Q.** Influence of Heat Treatment on Interface of Cu/Al Bimetal Composite Fabricated by Cold Rolling *Composite Part B-Engineering* 42 2011: pp. 1468–1473.
<https://doi.org/10.1016/j.compositesb.2011.04.045>
 30. **Hibino, A., Matsuoka, S., Kiuchi, M.** Synthesis and Sintering of Ni₃Al Intermetallic Compound by Combustion Synthesis Process *Journal Materials Processing Technology* 112 2001: pp. 127–135.
[https://doi.org/10.1016/S0924-0136\(01\)00558-1](https://doi.org/10.1016/S0924-0136(01)00558-1)
 31. **Sheng, L.Y., Yang, F., Guo, J.T., Xi, T.F.** Anomalous Yield and Intermediate Temperature Brittleness Behaviors of Directionally Solidified Nickel-based Superalloy *Transactions of Nonferrous Metals Society of China* 24 (3) 2014: pp. 673–681.
[https://doi.org/10.1016/S1003-6326\(14\)63110-1](https://doi.org/10.1016/S1003-6326(14)63110-1)
 32. **Du, B.N., Sheng, L.Y., Cui, C.Y., Yang, J.X., Sun, X.F.** Precipitation and Evolution of Grain Boundary Boride in A Nickel-based Superalloy during Thermal Exposure *Materials Characterization* 128 2017: pp. 109–114.
<https://doi.org/10.1016/j.matchar.2017.03.038>
 33. **Sheng, L.Y., Yang, F., Xi, T.F., Guo, J.T.** Investigation on Microstructure and Wear Behavior of the NiAl-TiC-Al₂O₃ Composite Fabricated by Self-propagation High-temperature Synthesis with Extrusion *Journal of Alloys and Compound* 554 2013: pp. 182–188.
<https://doi.org/10.1016/j.jallcom.2012.11.144>
 34. **Sheng, L.Y., Guo, J.T., Lai, C., Xi, T.F.** Effect of Zr Addition on Microstructure and Mechanical Properties of NiAl/Cr (Mo) Base Eutectic Alloy *Acta Metallurgica Sinica* 51 (7) 2015: pp. 828–834.
<https://doi.org/10.11900/0412.1961.2014.00610>
 35. **Li, C.Q., Xu, D.K., Wang, B.J., Sheng, L.Y., Qiao, Y.X., Han, E.H.** Natural Ageing Responses of Duplex Structured Mg-Li Based Alloys *Scientific reports* 7 2017: pp. 40078.
<https://doi.org/10.1038/srep40078>
 36. **Sheng, L.Y., Du, B.N., Wang B.J., Xu D.K., Lai, C., Guo, Y., Xi, T.F.** Hot Extrusion Effect on the Microstructure and Mechanical Properties of a Mg-Y-Nd-Zr Alloy *Strength of Materials* 50 (1) 2018: pp. 184–192.
<https://doi.org/10.1007/s11223-018-9958-9>
 37. **Zhang, W., Du, K., Chen, X.Q., Sheng, L.Y., Ye, H.Q.** Thermally Stable Coherent Domain Boundaries in Complex-Structured Cr₂Nb Intermetallics *Philosophical Magazine* 96 (1) 2016: pp. 58–70.
<https://doi.org/10.1080/14786435.2015.1125030>